JOURNAL OF GEOPHYSICAL RESEARCH, VOL. 107, NO. A7, 10.1029/2001JA900168, 2002

The dynamics of current carriers in standing Alfvén waves: Parallel electric fields in the auroral acceleration region

Andrew N. Wright
Mathematical Institute, University of St. Andrews, St. Andrews, Scotland, UK

W. Allan
National Institute of Water and Atmospheric Research, Wellington, New Zealand

Michael S. Ruderman
Department of Applied Mathematics, University of Sheffield, Sheffield, England, UK

R. C. Elphic
Los Alamos National Laboratory, Los Alamos, New Mexico, USA

Received 28 May 2001; revised 17 October 2001; accepted 20 October 2001; published 20 July 2002.

[1] The acceleration of current carriers in an Alfvén wave current system is considered. The model incorporates a dipole magnetic field geometry, and we present an analytical solution of the two-fluid equations by successive approximations. The leading solution corresponds to the familiar single-fluid toroidal oscillations. The next order describes the nonlinear dynamics of electrons responsible for carrying a few μAm^{-2} field aligned current into the ionosphere. The solution shows how most of the electron acceleration in the magnetosphere occurs within 1 R_E of the ionosphere, and that a parallel electric field of the order of 1 mVm^{-1} is responsible for energising the electrons to 1 keV. The limitations of the electron fluid approximation are considered, and a qualitative solution including electron beams and a modified $E_{||}$ is developed in accord with observations. We find that the electron acceleration can be nonlinear, $(v_{e||}\nabla_{||})v_{e||} > \omega v_{e||}$, as a result of our nonuniform equilibrium field geometry even when $v_{e||}$ is less than the Alfvén speed. Our calculation also elucidates the processes through which $E_{||}$ is generated and supported. *INDEX TERMS:* 7827 Space Plasma Physics: Kinetic and MHD theory; 2716 Magnetospheric Physics: Energetic particles, precipitating; 2451 Ionosphere: Particle acceleration; 2431 Ionosphere: Ionosphere/magnetosphere interactions (2736)

1. Introduction

[2] The details of how electrons are accelerated to high energies (keV) in the auroral region is still a matter of debate. Suggested acceleration mechanisms include the parallel electric fields generated by electric double layers [*Alfvén*, 1958], anomalous resistivity [*Swift*, 1975], kinetic Alfvén waves [*Hasegawa*, 1976], magnetic mirrors [*Knight*, 1973], and electrostatic shocks [*Mozer et al.*, 1977]. Another proposed mechanism is stochastic acceleration by lower hybrid electrostatic turbulence [*Bryant et al.*, 1991; *Bryant*, 1994]. The electrons carry intense field aligned currents whose origin is often not discussed in detail and relegated to a general generator region located some distance away.

[3] Field aligned currents, and the associated motion of electrons along magnetic field lines, are a basic feature of all magnetospheres. Before summarising previous contributions to this topic it is worth looking briefly at the basic properties of these electrons to help us focus on the salient points. Figure 1 shows electron and magnetic field data from the FAST satellite. The top panel shows the magnetic field component that is approximately aligned with the westward direction, so the field aligned current is upward for roughly the first half of the interval and switches sign for the second half. The lower panels show how the upward current is carried by a field aligned (0° pitch angle) motion of keV electrons. The downward current is carried by the dominant upward drift of electrons (180° pitch angle) of slightly less energy but greater density. It is clear that the electron motion is highly collimated, and it is the impact of the downward beam with the ionosphere that excites optical auroral emissions.

[4] Recently it has been shown that auroral emissions may be modulated by standing Alfvén waves on closed field lines, often referred to as field line resonances (FLRs) [*Samson et al.*, 1991, 1992, 1996; *Xu et al.*, 1993; *Liu et al.*, 1995]. The field aligned currents in these ultra-low-frequency (ULF) waves are carried by electrons that can also have keV energies. Since the theoretical model of these FLRs (with frequency a few mHz) is very well developed, understanding how they accelerate their electrons to such high energy may provide some basic understanding of the auroral acceration process in general.

0148-0227/02/2001JA900168$09.00

[5] The FLR approach has been taken recently by *Rankin et al.* [1999] who found that the mirror force would be important in producing large parallel electric fields ($E_{\|}$). They also noted that the convergence of field lines at high latitudes and associated increase in current density would also require large electron velocities, as did *Temerin and Carlson* [1998]. The scaling of the mean field aligned electron drift velocity as B/n was first recognised by *Swift* [1978], and was found to peak at an altitude of about 1 Earth radius by *Lysak and Hudson* [1979]. Moreover, observations are generally consistent with the maximum energization occurring in the vicinity of where B/n peaks. The importance of electron inertia in auroral currents was first noted by *Geortz and Boswell* [1979] which, together with the B/n scaling arguments, has led *Rönnmark* [1999] to claim that electron inertia alone can produce significant $E_{\|}$. (Rönnmark's model was not for FLRs, and assumed a prescribed equatorial mechanical force that drove the MHD current generator.)

[6] Many previous studies have employed the two-fluid approximation in which the electrons are described using a separate fluid to that of the ions. Indeed this is the obvious refinement to the well-established single-fluid MHD models of FLRs, and is the approach we adopt throughout most of this paper. The data in Plate 1 would indeed be described reasonably by a separate electron fluid, although the penetration of the downward electron beam into the ionosphere would be described better using a distribution function formulation. We discuss such situations qualitatively, and indicate the general features of the electron distribution function.

[7] Two-fluid models of FLRs in a dipole geometry have been presented by *Streltsov et al.* [1998] and references therein. The main focus of these papers was on nonradiative FLRs where the dispersion due to finite electron inertia (at high latitudes) is balanced by that associated with finite electron temperature (at low latitudes). Such an FLR must have a narrow width in L (the McIlwain magnetic shell parameter), and is likely to exist on the boundaries of auroral density cavities where steep gradients exist. Their model produces latitudinal widths of a few hundred metres at the ionosphere. *Wright and Allan* [1996] showed that phasemixing of linear FLRs in a "smooth" magnetosphere (with equilibrium scale lengths of several R_E) will occur too slowly compared to the ionospheric decay time for FLRs to narrow down to the electron inertia length. *Streltsov and Lotko* [1997] and *Streltsov et al.* [1998] also considered the electron energy and $E_{\|}$ of their solution. However, this was done linearly, and so is different from the treatment we present here.

[8] In the present paper we investigate Rönnmark's suggestion that electron inertia alone can generate significant parallel electric fields in the context of currents driven by FLRs. Observations show that in the acceleration region, a few thousand km above auroral arcs, number densities can be 10^6 m^{-3} or less [e.g., *Strangeway et al.*, 1998]. Typical FLR widths in the equatorial plane correspond to current sheets with a width between a quarter to a half of an Earth radius (R_E) which will map to between 25 to 50 km in the ionosphere. The typical FLR toroidal field above the ionosphere is of the order of 100 nT requiring parallel current densities of a few μAm^{-2} to be carried by electrons with velocities of 2×10^7 m s^{-1}, i.e., having keV energies. Our calculation shows that in a dipole field $E_{\|}$ increases dramatically above the auroral arcs, reaching a few mVm^{-1} in a location consistent with what is commonly referred to as the accelerator region. Not only can electron inertia give rise to values of $E_{\|}$ consistent with observation, but it also provides a natural explanation for the location of the principal accelerator region.

[9] In our modeling we employ a dipole equilibrium field, and adopt the following numerical values which are consistent with the observations mentioned above. Optical auroral emission modulation is observed at latitudes of 70° to 72°, and we take the $L = 10$ field line to be typical of this region (the invariant latitude is $\Lambda = 71.54°$). At $L = 10$ an FLR half-width of 0.25 R_E in the equatorial plane maps to 25 km in the ionosphere. The equilibrium field strength at the ionospheric end of the field line is taken as 5×10^4 nT, which corresponds to 25 nT in the equatorial plane.

[10] Typical FLR frequencies lie in the range 1–4 mHz [*Samson et al.*, 1991, 1992, 1996], and we adopt a value of 2 mHz as being typical. The amplitude of the Alfvén wave may be expressed in terms of the radial electric field (1 mVm^{-1}) or the azimuthal $\mathbf{E}_{\wedge}\mathbf{B}$ drift velocity (50 km s^{-1}) in the equatorial plane. For our constant density ($n = 10^6$ m^{-3}) model this corresponds to an FLR azimuthal magnetic field of 100 nT just above the ionosphere, and a parallel current density of 2 μAm^{-2} given the cross L-shell scale mentioned above.

[11] The wave frequency of 2 mHz in a dipole field is shown (in the appendix) to require an equatorial Alfvén speed of 400 km s^{-1}. Since we assume $n = 10^6$ m^{-3}, this implies a mean ion mass of 1.9 a.m.u., indicating the presence of 6% oxygen. We also note that the departure of the true equilibrium field from a dipole can also affect the frequency.

2. Governing Equations

[12] In sections 2, 3, and 4 we assume a cold two-fluid plasma model which is charge neutral ($n_e = n_i = n$) and denote the electron and ion charge in terms of e ($q_i = -q_e = e$). The equations of motion for the electron and ion fluids are

$$nm_e\left(\frac{\partial \mathbf{v}_e}{\partial t} + (\mathbf{v}_e \cdot \boldsymbol{\nabla})\mathbf{v}_\mathbf{e}\right) = -ne(\mathbf{E} + \mathbf{v}_{e\wedge}\mathbf{B}) \tag{1}$$

$$nm_i\left(\frac{\partial \mathbf{v}_i}{\partial t} + (\mathbf{v}_i \cdot \boldsymbol{\nabla})\mathbf{v}_i\right) = ne(\mathbf{E} + \mathbf{v}_{i\wedge}\mathbf{B}) \tag{2}$$

where $\mathbf{v}_i$ and $\mathbf{v}_e$ are the ion and electron fluid velocities, respectively. $\mathbf{E}$ and $\mathbf{B}$ are the electric and magnetic fields which obey Ampère's law and Faraday's law,

$$\boldsymbol{\nabla}_{\wedge}\mathbf{B} = \mu_o\mathbf{j} \tag{3}$$

$$\boldsymbol{\nabla}_{\wedge}\mathbf{E} = -\frac{\partial \mathbf{B}}{\partial t} \tag{4}$$

The current density is

$$\mathbf{j} = ne(\mathbf{v}_i - \mathbf{v}_e) \tag{5}$$

It is useful to discuss part of the solution in terms of the single fluid approximation, and we define the center of mass velocity $\mathbf{v}$ and plasma mass density ρ by

$$\rho = n(m_e + m_i) \tag{6}$$

$$\mathbf{v} = \frac{m_e\mathbf{v}_e + m_i\mathbf{v}_i}{m_e + m_i} \tag{7}$$

The equations of continuity for each species, $\partial n_s/\partial t + \nabla\cdot(n_s\mathbf{v}_s) = 0$, may be added in the quasi-neutral approximation to give

$$\frac{\partial\rho}{\partial t} + \nabla\cdot(\rho\mathbf{v}) = 0 \tag{8}$$

The standard single fluid treatment does not solve for $\mathbf{v}_e$ and $\mathbf{v}_i$ but works with the sum and difference expressed via $\mathbf{v}$ and $\mathbf{j}$: Adding the equations of motions equation (1) and (2) yields the single fluid equation of motion (retaining electron inertia)

$$\rho\left(\frac{\partial\mathbf{v}}{\partial t} + (\mathbf{v}\cdot\nabla)\mathbf{v}\right) + \frac{m_e m_i}{e^2(m_e + m_i)}(\mathbf{j}\cdot\nabla)(\mathbf{j}/n) = \mathbf{j}_\wedge\mathbf{B} \tag{9}$$

Traditionally, the species equations of motion (1) and (2) are multiplied by their respective charges and divided by their masses, then added to give the generalised Ohm's law (relating $\mathbf{E}$, $\mathbf{B}$, and $\mathbf{j}$). We prefer not to follow this procedure, since it eliminates $\mathbf{v_e}$, and this quantity is not only easy to observe but directly related to $E_\parallel$. Working with $\mathbf{v}$, $\mathbf{v_e}$, and $\mathbf{j}$ allows us to derive the familiar single fluid solution, but also study the electron dynamics and the associated $E_\parallel$.

[13] We begin by eliminating $\mathbf{v}_i$ from the equations. Combining equations (5) and (7) gives

$$\mathbf{j} = ne\left(1 + \frac{m_e}{m_i}\right)(\mathbf{v} - \mathbf{v}_e) \tag{10}$$

The above relation is then used to substitute for $\mathbf{v}_e$ in the right hand side only of equation (1) giving us an alternative formulation of Ohm's law,

$$m_e\left(\frac{\partial\mathbf{v}_e}{\partial t} + (\mathbf{v}_e\cdot\nabla)\mathbf{v}_e\right) = -e(\mathbf{E} + \mathbf{v}_\wedge\mathbf{B}) + \frac{1}{n}\left(1 + \frac{m_e}{m_i}\right)^{-1}\mathbf{j}_\wedge\mathbf{B} \tag{11}$$

Substituting for $\mathbf{v_e}$ in terms of $\mathbf{v}$ and $\mathbf{j}$ on the left hand side also (using equation (10)) would give the standard representation of Ohm's law.

3. Solution Method

[14] We solve the above equations by successive approximations to the full solution using regular perturbation theory. The equilibrium magnetic field is assumed to be axisymmetric and current-free. An orthogonal curvilinear coordinate system (ν, ϕ, μ) is used in which ν labels L shells, ϕ is the azimuthal coordinate, and μ is a field aligned coordinate. The perpendicular electric field is taken to be zero at the ionosphere, and all wave fields are axisymmetric ($\partial/\partial\phi = 0$). Later we shall evaluate a solution explicitly for the dipole coordinate system, but for the moment we keep the discussion general.

3.1. Single Fluid Solution

[15] We begin by deriving a solution that is known to work well for the basic FLR structure we are interested in. The magnetic amplitude of an FLR is typically 5% of the equilibrium magnetic field value, so we begin by neglecting nonlinear terms and also m_e compared to m_i. We also note that the magnitude of the $\mathbf{j}_\wedge\mathbf{B}$ term in our Ohm's law equation (11) scales as the ratio of the wave frequency (ω) to the ion cyclotron frequency (ω_{ci}), and will be much less than 1 for ULF FLRs. Within these approximations the linear velocity and magneftic fields ($\mathbf{v}$ and $\mathbf{B}$, respectively) satisfy

$$\rho_0\frac{\partial\mathbf{v}}{\partial t} = (\nabla_\wedge\mathbf{B})_\wedge\mathbf{B}_0/\mu_o \tag{12}$$

$$\frac{\partial\mathbf{B}}{\partial t} = \nabla_\wedge(\mathbf{v}_\wedge\mathbf{B}_0) \tag{13}$$

(ρ_0 and $\mathbf{B}_0$ denote equilibrium quantities.)

[16] The axisymmetric solutions to these equations are toroidal Alfvén waves with only the ϕ components nonzero. Each L shell oscillates independently at its own natural frequency which may be solved for (along with the fields themselves) by integration along each field line. It is the tendency for each field line to oscillate with a distinct natural frequency, $\omega_A(\nu)$, that leads to phasemixing and the growth of large currents in an undriven solution or the selection of a resonant field line with large currents in the cavity or waveguide model [*Wright*, 1994a, 1994b; *Mann et al.*, 1995].

[17] The current in this Alfvén wave solution may be expressed in terms of the geometric scale factors h_ν, h_ϕ, and h_μ.

$$\mathbf{j} = \frac{1}{\mu_o}\left(\frac{-1}{h_\phi h_\mu}\frac{\partial(h_\phi b_\phi)}{\partial\mu}, 0, \frac{1}{h_\nu h_\phi}\frac{\partial(h_\phi b_\phi)}{\partial\nu}\right) \tag{14}$$

[18] The Alfvén wave solution above corresponds to each L shell oscillating in the toroidal direction with velocity v_ϕ, and this motion bends the field line giving rise to b_ϕ. The above equation shows how this field is associated with a current in the ν-direction (across L shells) and the μ-direction (the field aligned direction): It is the $\mathbf{j}_\wedge\mathbf{B}_0$ force of the j_ν current that provides the force to move the single fluid plasma in the ϕ direction. The $j_\parallel$ current produces no force, but is required to keep $\nabla\cdot\mathbf{j} = 0$. Under the approximations used in this section Ohm's law reduces to

$$\mathbf{E} + \mathbf{v}_\wedge\mathbf{B}_0 = 0 \tag{15}$$

so the Alfven wave electric field is strictly in the ν-direction. $E_\parallel$ is zero in this solution.

3.2. Currents and Charge Carriers

[19] We now return to the motion of electrons and ions to see how the current required in equation (14) is carried.

Returning to equations (1) and (2), we take their cross product with **B** to get

$$\mathbf{v}_{e\perp} = \mathbf{E}_\wedge\mathbf{B}/B^2(1 + \mathrm{O}(\omega/\omega_{ce})) \quad (16)$$

$$\mathbf{v}_{i\perp} = \mathbf{E}_\wedge\mathbf{B}/B^2(1 + \mathrm{O}(\omega/\omega_{ci})) \quad (17)$$

These equations show that to a very high order electrons drift with a velocity $\mathbf{E}_\wedge\mathbf{B}/B^2$, and this corresponds to v_ϕ in the previous section. The ion motion is also dominated by this drift, but there is a more significant departure from it than in the case of the electrons. This is a restatement of the calculation of a ''field line velocity'' (**w**) by *Dungey* [1958], where he shows

$$\mathbf{w} = \frac{m_i\mathbf{v}_e + m_e\mathbf{v}_i}{m_i + m_e} \quad (18)$$

indicating that the field lines are frozen in to the electron fluid to a much higher degree than to the ion fluid (by a factor of m_i/m_e). The small drift of the ions can be considered as a correction to the solution in the previous subsection by returning to the full Ohm's law equation (11) and taking its vector product with **B**

$$\mathbf{v}_\perp = \mathbf{E}_\wedge\mathbf{B}/B^2 + \frac{1}{ne(1 + m_e/m_i)}\mathbf{j}_\perp(1 + \mathrm{O}(m_e/m_i)) \quad (19)$$

The small error in this equation arises from the neglect of the left hand side of equation (11) relative to the term involving **j**. The above equation shows clearly how the perpendicular current in equation (14) is carried by a small drift of the single fluid plasma in the ν-direction, which can be shown to be a factor of ω/ω_{ci} smaller than the $\mathbf{E}_\wedge\mathbf{B}$ drift. Of course, from equation (7), this is essentially just the drift of ions (in accord with the expected correction indicated in equation (17)). Over one cycle the trajectory of the ions is an ellipse whose major axis is aligned with the ϕ direction. The ratio of minor to major axes is ω/ω_{ci}. The electrons also have a drift in the ν direction, but smaller by a factor of m_e/m_i than the ion drift. The motion of ions in the ν-direction in a collisionless plasma is a result of the oscillating Alfvén wave electric field (E_ν) and scales as ω/ω_{ci}. The current associated with this drift is called the polarization current and produces the $\mathbf{j}_\wedge\mathbf{B}$ term in Ohm's law equation (11).

[20] The parallel motion of charge carriers may be examined by taking the scalar product of **B** with the momentum equations: Applying this to the linearized form of equation (9) gives $\rho_o\partial\mathbf{v}_\parallel/\partial t = 0$, so there is no motion of the single fluid along the background field. The electron and ion momentum equations (1) and (2) yield

$$m_e\left(\frac{d\mathbf{v}_e}{dt}\right)\cdot\mathbf{B} = -e\mathbf{E}\cdot\mathbf{B} \quad (20)$$

$$m_i\left(\frac{d\mathbf{v}_i}{dt}\right)\cdot\mathbf{B} = e\mathbf{E}\cdot\mathbf{B} \quad (21)$$

The field aligned acceleration of electrons is greater than that of the ions by a factor of m_i/m_e. Thus electrons are much more mobile than ions along the magnetic field and are the dominant carriers of field aligned currents: The parallel component of equation (10) gives

$$j_\parallel = -ne\left(1 + \frac{m_e}{m_i}\right)v_{e\parallel} \quad (22)$$

and to leading order in m_e/m_i is just the current carried by the electrons, as expected. Figure 2 shows a sketch of the current circuit in a fundamental standing Alfvén wave, at one instant. The current and particle drifts oscillate with the Alfvén wave frequency, so half a cycle later the directions of these quantities will be reversed. The field aligned currents are carried by electrons. As the current approaches the equatorial section an increasing amount of the field aligned current is diverted across field lines as the polarization current (carried by ions, see equation (19)). Naturally, this current circuit is divergence free. Notice also that charge neutrality is preserved: The divergence of electrons from the equatorial region (along the field line) is matched by an equal divergence of ions (across the field lines). Although we do not discuss the interaction with the ionosphere in detail in this paper, we note the parallel current is closed by a transverse ionospheric Pedersen current carried by ions.

3.3. Generation of Field-Aligned Current

[21] The mechanism through which the ''generator region'' produces $j_\parallel$ and $v_{e\parallel}$ can now be identified. Frequently the acceleration of electrons is discussed in terms of an $E_\parallel$ associated with kinetic Alfvén waves or electron inertial Alfvén waves. However, this cannot account for the fact that broad FLRs have scales much larger than the electron inertial length and ion gyroradius, yet still manage to have $j_\parallel \sim \mu\mathrm{Am}^{-2}$ carried by keV energy electrons.

[22] The flow chart in Figure 3 delineates our conceptual framework, which is similar to that of *Nakamura* [2000], and draws onbasic concepts from electromagnetism. The first box determines $\mathbf{j}_\perp$ from the single-fluid momentum equation. The detailed calculation presented elsewhere in this paper is based upon the polarization current associated with the inertial term, although a more general consideration would include gradients in pressure (p) and other mechanical body forces (**F**).

[23] Since we are interested in how $\mathrm{j}_\parallel$ is generated, we shall assume $j_\parallel = 0$ initially and show that it is normally impossible to avoid the subsequent growth of $j_\parallel$. When $j_\parallel = 0$, $\nabla\cdot\mathbf{j} \equiv \nabla\cdot\mathbf{j}_\perp$ which is generally nonzero, and leads to the charge density ($\rho^* = (n_i - n_e)e$) becoming nonzero too since $\partial\rho^*/\partial t + \nabla\cdot\mathbf{j} = 0$. (For the polarization current described above this is due to the convergence or divergence of ion drifts across L-shells.) If $j_\parallel$ remained zero throughout the Alfvén wave cycle ρ^* would reach $\sim 10^{-16}$ Cm^{-3} in the equatorial plane for the parameters given in the introduction. This is equivalent to $(n_i - n_e)/n \sim 10^{-3}$, and represents a violation of quasi-neutrality. Indeed, if this situation could be realised $\nabla\,\mathbf{E} = \rho^*/\epsilon_o$ suggests electric fields of several hundreds of mVm^{-1} would exist. Of course, ρ^* and **E** never grow to this extent because the electric fields that are produced generally have a nonzero $E_\parallel$ which accelerates electrons along **B** in such a way that ρ^* is reduced and the plasma remains quasi-neutral. From this point of view we could say that $j_\parallel$ evolves in order that $\nabla\cdot\mathbf{j} \approx 0$, i.e., the plasma remains quasi-neutral ($\rho^* \approx 0$). The plasma is

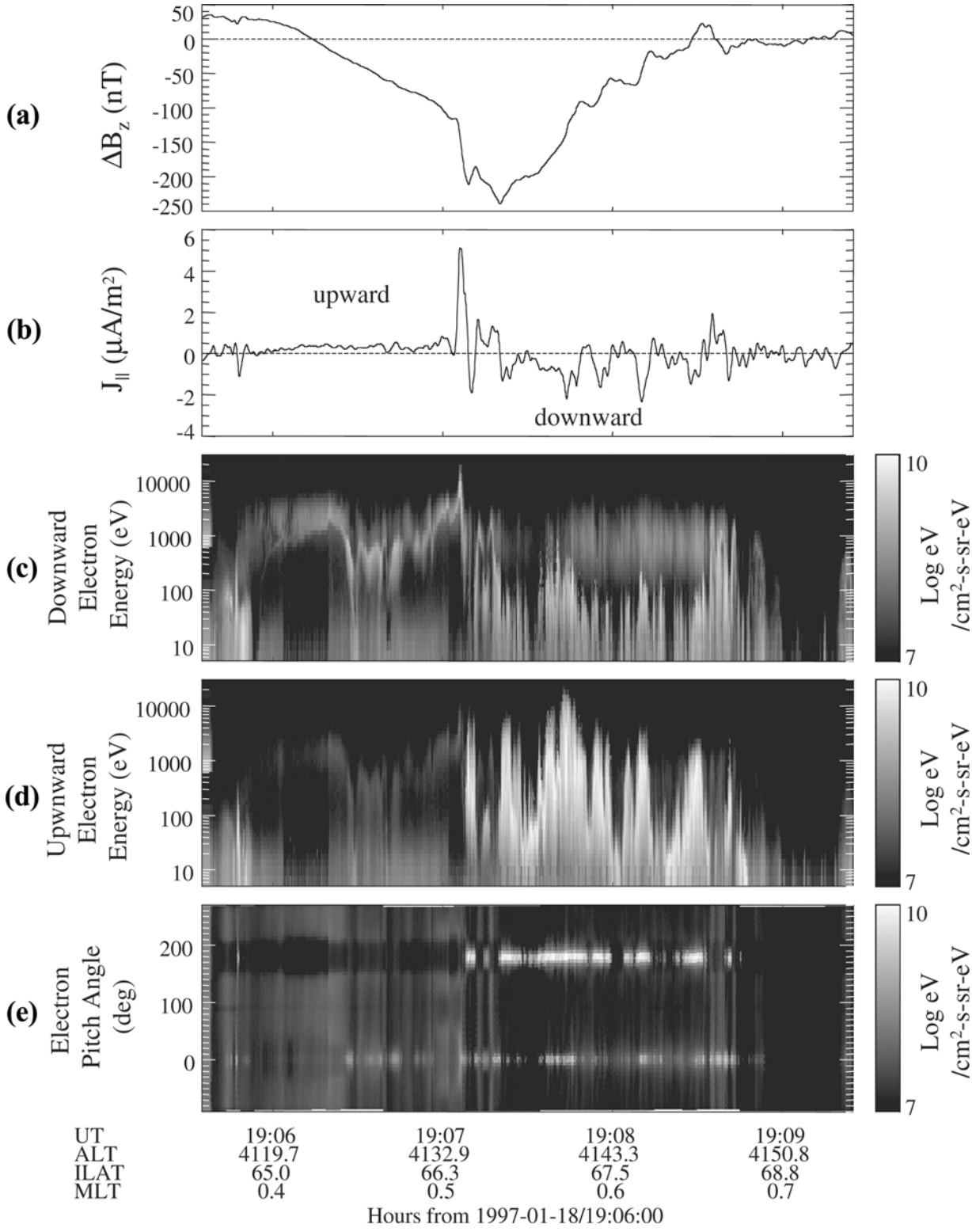

Figure 1. FAST observations of a field aligned auroral current system crossing near midnight. (a) The spin axis component (nearly westward) of the magnetic field. A positive (negative) slope indicates downward (upward) current. (b) The (upward) field aligned current density. (c, d) The energy spectrograms for downgoing and upgoing electrons. (e) The electron pitch angle distribution. Electrons near 0° are downgoing.

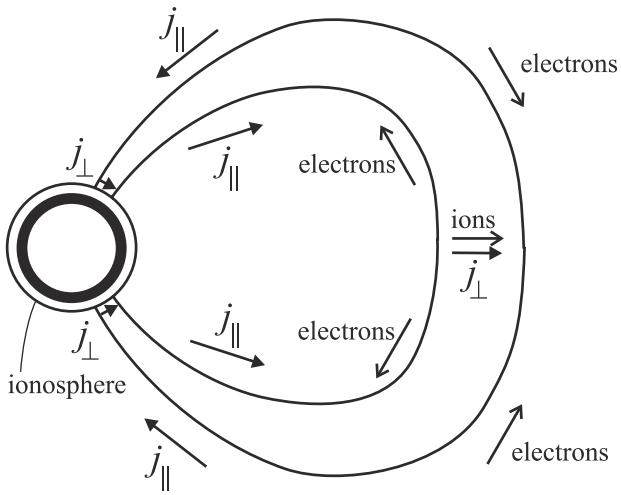

Figure 2. The current circuit in a standing Alfven wave. The field aligned currents are carried predominantly by electrons, whereas the polarization and Pedersen currents are carried by ions. Half a cycle later the currents will be reversed.

not *exactly* neutral, and the small deviation from neutrality ($\rho^* \neq 0$) is sufficient to account for the divergence of the wave's **E** field. Note that **E** has an $\mathbf{E}_\perp$ associated with single-fluid $\mathbf{E}_\wedge\mathbf{B}$ drift and an $E_\parallel$ that is required to accelerate the electrons to carry the necessary $j_\parallel$ that will maintain $\nabla \cdot \mathbf{j} \approx 0$.

[24] These results are to be expected since the Debye length in the magnetosphere is a few hundred metres, and the plasma will be quasi-neutral on scales larger than this. In fact for our FLR the **E** fields we require are associated with densities of $(n_i - n_e)/n \sim 10^{-8}$ at the equatorial plane, and 10^{-5} in the accelerator region. Thus the plasma remains quasi-neutral. This approximation is also reflected by the neglect of the displacement current in equation (3): Taking the divergence of the full equation yields

$$\nabla \cdot \mathbf{j} = -\epsilon_o \frac{\partial \nabla \cdot \mathbf{E}}{\partial t} \equiv -\frac{\partial \rho^*}{\partial t} \tag{23}$$

the final term originating from the displacement current. The neglect of the displacement current density in equation (3) is a good approximation for our solution, it being less than the conduction current density by between 10^{-6} and 10^{-9} over the length of the field line.

4. Parallel Electric Fields and Electron Dynamics

[25] *Bryant et al.* [1992] note that electrostatic potential acceleration processes cannot provide a suitable accelerator of auroral electrons as they require unphysical sources or sinks of charged particles. Although this criticism does not apply to our model (which is based upon an oscillatory wave), it may be that the observed current would drain the flux tube of charge carriers in less than a wave period, which would lead to a breakdown of our model.

4.1. Drainage Time

[26] Let us consider a worst case scenario for the drainage of a flux tube by a parallel current: We shall assume that n is constant along the flux tube, and does not increase at high latitudes. The magnetic flux of a tube is constant along its length,

$$A(\mu)B(\mu) = \text{const.} \tag{24}$$

where the cross sectional area of the flux tube is $A(\mu)$. Recall that μ is the field aligned coordinate, and varies between 0 and μ_i from the equator to the ionosphere. An element of path length along the field line is equal to $h_\mu d\mu$ (see the appendix for the dipole expressions of h_μ and other quantities) so the volume of the flux tube is

$$V = \int_0^{\mu_i} A(\mu) h_\mu d\mu \tag{25}$$

and the number of electrons it contains is $N = nV$. Suppose electrons leave the ionospheric end of the flux tube at a speed $v_{e\parallel}(\mu_i)$, then the flux of electrons leaving the tube is

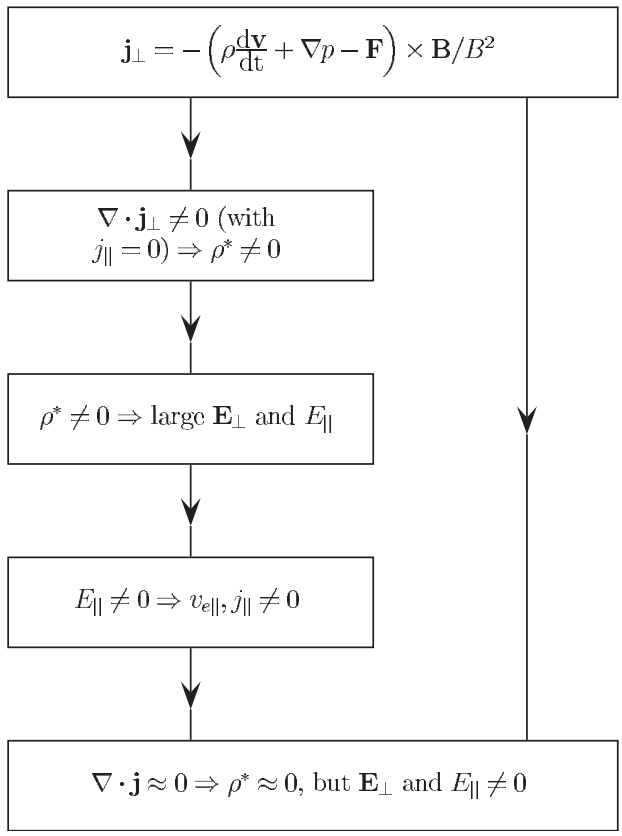

Figure 3. A flow chart identifying the concepts describing the generation of field-aligned currents: $\mathbf{j}_\perp$ (identified from the momentum equation) will, in the absence of $j_\parallel$, lead to a net charge density (ρ^*), and from Gauss's Law will be associated with electric fields. The $E_\parallel$ component acts to move electrons along **B** and short out the accumulated charge density, i.e., a field-aligned current is generated. The combination of $j_\parallel$ and $\mathbf{j}_\perp$ keep the plasma quasi-neutral. The small deviation from neutrality and the wave's **E** field balance in Gauss's Law.

$nv_{e\|}(\mu_i)A(\mu_i)$, and the time to empty the flux tube of electrons is

$$\tau = \frac{V}{v_{e\|}(\mu_i)A(\mu_i)} \tag{26}$$

Combining the above with relations for a dipole geometry (see the appendix), and using the latitude (θ) and invariant latitude (Λ) gives

$$\tau = \frac{LR_E}{v_{e\|}(\Lambda)} \frac{\sqrt{1+3\,\sin^2\Lambda}}{\cos^6\Lambda} \int_0^\Lambda \cos^7\theta d\theta \tag{27}$$

Evaluating the integral for $L = 10$ ($\Lambda = 71.5$) for 1 keV electrons ($v_{e\|} = 2 \times 10^7$ m s^{-1}) gives a drainage time of about 50 min. A 2 mHz FLR has a period (T) of about 8 min over which time the parallel current oscillates. We could estimate the effective loss of electrons by saying that electrons leave at the maximum rate for just a quarter of a cycle (2 min), meaning that less than 5% of the electrons would be removed from the flux tube. As we stated above, this is a worst case scenario because (1) we considered the fundamental mode. Higher harmonics will empty the flux tubes for shorter times. (2) We assumed the number density to be constant ($n = 10^6$ m^{-3}) along the field line. (3) We considered the emptying of a flux tube, and not the filling from ionospheric electrons. In the above example it would be sufficient to have a 2.5% enhancement of the equilibrium number density during the downward current phase of the cycle, and 2.5% decrease from the equilibrium during the upward current phase. Given these considerations, it appears that we will not need to postulate any unphysical sources or sinks of particles.

4.2. Parallel Electric Fields

[27] We now return to the question of electron acceleration in our single fluid solution. Given the Alfvén wave b_ϕ perturbation we can calculate the field aligned current component in equation (14) and this tells us directly what $v_{e\|}$ is from equation (22). The perpendicular motion of the electrons is just the $\mathbf{E}_\wedge\mathbf{B}$ drift (i.e., the v_ϕ motion of the Alfvén wave) to a very high degree equation (16). Thus, given the Alfvén wave solution we can calculate the electron velocity $\mathbf{v}_e = (0, v_{e\phi}, v_{e\|})$.

[28] The parallel ($\hat{\mu}$) component of Ohm's law equation (11) gives

$$m_e\left(\frac{\partial \mathbf{v}_e}{\partial t} + (\mathbf{v}_e\cdot\boldsymbol{\nabla})\mathbf{v}_e\right)\cdot\hat{\mu} = -eE_\|\tag{28}$$

Note that the leading order (linear) solution derived in section 3 had $E_\|$ identically zero equation (15). The successive approximation to $E_\|$ we calculate now shows that although $E_\|$ is small, it is not actually zero.

[29] Evaluating the parallel component of the convective derivative in equation (28) requires some care and is facilitated by using the identity $(\mathbf{v}_e\cdot\boldsymbol{\nabla})\mathbf{v}_e = (\boldsymbol{\nabla}_\wedge\mathbf{v}_e)_\wedge\mathbf{v}_e + \boldsymbol{\nabla}(v_e^2/2)$. For our axisymmetric solution we get, after some algebra,

$$E_\| = -\frac{m_e}{e}\left(\frac{\partial v_{e\|}}{\partial t} + \frac{v_{e\|}}{h_\mu}\cdot\frac{\partial v_{e\|}}{\partial\mu} - \frac{v_{e\phi}^2}{h_\mu}\cdot\frac{\partial \ln h_\phi}{\partial\mu}\right)\tag{29}$$

Note that the expression for the field aligned acceleration (in parentheses above) is different to the approximation employed in *Streltsov and Lotko* [1997]. The term in $v_{e\phi}$ represents the centripetal acceleration resolved in the $\hat{\mu}$ direction. It is useful to consider the relative magnitudes of the three acceleration terms for the parameters given in the introduction. Consider the time derivative and centripetal terms first. The scale on which h_ϕ varies is that of the equilibrium field, and 1 R_E can be regarded as a safe lower limit. For these terms to have a similar magnitude in a μAm^{-2} current requires $v_{e\phi}$ to be of order 2000 km s^{-1}, which is greater than observed values at high latitudes by two or three orders of magnitude. Thus, the centripetal acceleration is unlikely to be important in the accelerator region.

[30] Now consider the magnitudes of the time derivative and the field aligned convective derivative $(v_{e\|}\nabla_\|)v_{e\|}$ for the typical quantities we quoted in the introduction that are representative of the high latitude section of the field line. If the length along the field line over which $v_{e\|}$ changes is $\ell_\|$, then the $\partial v_{e\|}/\partial t$ term is much less than the $(v_{e\|}\nabla_\|)v_{e\|}$ term unless $\ell_\|$ exceeds 250 R_E. Since this is over 10 times the length of the field line (and hundreds of times the length of the likely acceleration section) we can be confident that the convective term in equation (29) will dominate at high latitudes where $E_\|$ is significant. In this region we have

$$E_\| \approx -\frac{m_e}{e}(v_{e\|}\nabla_\|)v_{e\|}\tag{30}$$

It is interesting to note that although the Alfvén wave solution (v_ϕ, b_ϕ, $\mathbf{j}$, E_ν) is a linear solution, the dearth of charge carriers at high latitudes means that the electron velocity must be very large (2×10^7 m s^{-1}) to carry the current, and this means that the electron dynamics are nonlinear, as demonstrated in equation (30). The leading linear solution of section 3 remains valid because the ion velocity remains linear and $\mathbf{v} \approx \mathbf{v}_i$ despite $\mathbf{v}_e$ being nonlinear.

[31] It is often considered that electron inertia alone cannot provide the required $E_\|$: Observations suggest that acceleration occurs over a length of about 1 R_E, and for 1 keV electrons equation (30) implies $E_\|$ will be of the order of 1 mVm^{-1} which is also consistent with commonly inferred values. Since $E_\| \propto v_{e\|}^2 \propto j_\|^2 \propto b_\phi^2$, increasing the amplitude of the Alfvén wave by a factor of 3 will produce electrons with energies of 10 keV and $E_\|$ of 10's of mVm^{-1}.

[32] Models which treat the electron motion linearly will underestimate $E_\|$ in FLRs by a factor of 10^3 as they normally estimate the acceleration to be $\partial v_{e\|}/\partial t$ rather than $(v_{e\|}\nabla_\|)v_{e\|}$ (see also the estimate of *Rankin et al.*, [1999]). This statement is supported by the analysis in *Streltsov and Lotko* [1996] where they noted that the neglect of the convective derivative was questionable even in a box model, for which the field geometry does not cause a significant increase in current density at high latitudes.

[33] The strong convergence of magnetic field lines yields a short FLR scale across L-shells in the ionosphere. For example, the full width of the current sheet ($2\ell_\nu$) can be as small as 50 km. It is interesting to compare this scale with the electron inertia length $\ell_e = c/\omega_{pe}(\omega_{pe}^2 = ne^2/(m_e\epsilon_o))$, since *Wei et al.* [1994] and *Wright and Allan* [1996] note that neglect of two-fluid terms from the leading-order single fluid solution begins to become significant when $2\ell_\nu \approx 10\ell_e$.

The electron inertia length based upon an ionospheric number density of 10^{10} m^{-3} is ℓ_e = 50 m, which is a thousand times less than the FLR scale, so the leading single fluid solution should be accurate. If the ionospheric plasma has been evacuated ($n = 10^6$ m^{-3}) ℓ_e = 5 km, which is one tenth of the minimum FLR scale. Two-fluid effects associated with this scale are only just beginning to manifest themselves so we do not expect the leading single fluid solution to require significant revision in this case [*Wei et al.*, 1994; *Wright and Allan* 1996].

4.3. Analytical Model

[34] Whilst the estimates of the previous section are plausible, we have assumed, in accord with observations, that there is a short section (of about 1 R_E) of the field line at high latitudes where the acceleration occurs. No explanation was given for the size or location of this region. To support the ideas described above, we use an analytical solution for FLRs in a dipole field geometry (developed by *Taylor and Walker* [1984]) for a uniform density distribution of $n = 10^6$ m^{-3}. The details are given in the appendix, and here we only state the expressions for the field aligned variation of the two nonzero electron velocity components.

$$v_{e\|} \propto \frac{\sqrt{1+3\sin^2\theta}}{\cos^6\theta}\left[\cos\left(\frac{\pi s}{s_0}\right)+\left(\frac{3\eta_{13}}{9\eta_{11}-8}\right)\cos\left(\frac{3\pi s}{s_0}\right)\right] \quad (31)$$

$$v_{e\phi} \propto \cos^3\theta\left[\sin\left(\frac{\pi s}{s_0}\right)+\left(\frac{\eta_{13}}{9\eta_{11}-8}\right)\sin\left(\frac{3\pi s}{s_0}\right)\right] \quad (32)$$

where $s = \sin\theta + \sin\Lambda$ and $s_0 = 2\sin\Lambda$. For an $L = 10$ field line $\Lambda = 71.54°$, and in our constant density equilibrium $\eta_{11} = 0.393237$ and $\eta_{13} = 0.318194$. The upper panel of Figure 4 shows a plot of the velocity components as a function of distance along the field line from the equator ($\ell = 0$) to the northern ionosphere. $v_{e\|}$ has been normalised to be 2×10^7 m s^{-1} at the ionosphere (appropriate for 1 keV electrons) and $v_{e\phi}$ has an amplitude of 5×10^4 m s^{-1} at the equator (appropriate for a large FLR). Both $v_{e\|}$ and $v_{e\phi}$ oscillate with the frequency of the linear Alfvén wave although they are out of phase by $\pi/2$.

[35] It is instructive to compare the ratio of $(v_{e\|}\nabla_\|)v_{e\|}$ to $\partial v_{e\|}/\partial t$ for a 2 mHz wave given the $v_{e\|}$ variation in Figure 4. Denoting the wave frequency by ω and the local parallel length scale of $v_{e\|}$ by $\ell_\|$, the ratio of the two terms may be written as

$$\frac{(v_{e\|}\nabla_\|)v_{e\|}}{\omega v_{e\|}} \approx \frac{v_{e\|}}{\omega\ell_\|} \equiv \frac{v_{e\|}}{V_A}\cdot\left(\frac{V_A}{\omega\ell_\|}\right), \quad (33)$$

V_A being the local Alfvén speed. The lower panel in Figure 4 displays the variation of $v_{e\|}/V_A$ as a triple-dot dash line. Consider for a moment a uniform medium in which the parallel scale length of $v_{e\|}$ will simply be the parallel Alfvén wavelength, which is equal to V_A/ω. Thus the term in parentheses in equation (33) is of the order of unity suggesting that when $v_{e\|} < V_A$ the time derivative dominates the convective derivative. This is the type of behavior we expect over the equatorial section of the field line where the equilibrium is uniform to first order. However, this need not be the case in a nonuniform medium because $\ell_\|$ can be very different to the notional Alfvén wavelength V_A/ω. For example, at the high latitude section of the flux tube $\ell_\|$ is determined by the scale of the equilibrium field, which is much smaller than V_A/ω. Thus the convective term dominates the time derivative term if

$$\frac{v_{e\|}}{V_A} > \frac{\omega\ell_\|}{V_A} \quad (34)$$

The right-hand side of equation (34) can be considerably less than 1 and provides a condition that we show in the next section can be easily satisfied at high latitudes.

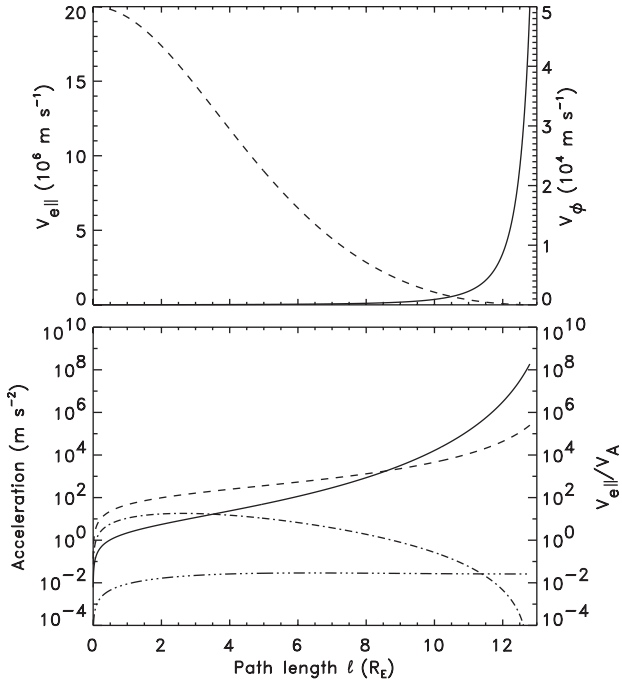

Figure 4. (top) The variation of the parallel electron velocity along a constant density $L = 10$ field line from the equator ($\ell = 0$) to the northern ionosphere (solid line). The field aligned variation of the ϕ component of the electron velocity is plotted as a dashed line. (bottom) The field aligned variation of the three electron acceleration terms in (29) for a 2 mHz wave at $L = 10$: $(v_{e\|}\nabla_\|)v_{e\|}$ (solid line), $\omega v_{e\|}$ (dashed line), and $v_{e\phi}^2\nabla_\|$ ln h_ϕ (dot-dashed line). The ratio of $v_{e\|}$ to V_A is shown as a triple dot-dashed line.

5. Discussion

5.1. Nonlinear Electron Dynamics

[36] Notice from the upper panel of Figure 4 that $v_{e\|}$ increases dramatically as the ionosphere is approached. The speed increases by a factor of e over about the last 1 R_E, and this may explain the approximate location of the "accelerator region." Electrons enter this region with 0.1 keV energy and emerge from it with 1 keV energy. The plot of $v_{e\phi}$ shows the expected antinode at the equator and node at the ionosphere. If the equilibrium field had been uniform, $v_{e\phi}$ would be a cosine curve. The dipolar geometry causes a marked decrease in $v_{e\phi}$ at high latitudes due to the convergence of field lines.

[37] We are now in a position to calculate the acceleration terms on the right hand side of equation (29) explicitly using the exact solution which is plotted in the upper panel of Figure 4. The lower panel of Figure 4 is a logarithmic plot of $(v_{e\|}\nabla_\|)v_{e\|}$ (solid line), $\omega v_{e\|}$ (dashed line), and the centripetal term $v_{e\phi}^2\nabla_\|$ ln h_ϕ (dot-dashed line). As expected from the discussion in section 4.3, $(v_{e\|}\nabla_\|)v_{e\|}$ dominates at high latitudes where $v_{e\|}$ is large and varies over a small length scale. The $\omega v_{e\|}$ term dominates at low latitudes where $v_{e\|}$ is small compared to V_A and the equilibrium is quasi-uniform. The centripetal acceleration never seems to be significant. For the last 4 R_E of the field line the magnitude of $(v_{e\|}\nabla_\|)v_{e\|}$ dominates that of $\omega v_{e\|}$ by up to a factor of 1000. Evaluating $E_\|$ according to equation (30) at the end of the field line gives a parallel electric field of 1 mVm^{-1}. Thus the analytical solution we have presented fully supports the qualitative discussion and ideas developed in the previous section. The triple-dot dash line in Figure 4 shows that the quantity $v_{e\|}/V_A$ is approximately constant, except near $\ell = 0$, where $v_{e\|}$ has a node. This property is not surprising since $v_{e\|} \propto j_\|/n$, and as *Rönnmark* [1999] notes, $j_\| \propto B$, suggesting $v_{e\|} \propto B/n$. Of course, $V_A \propto B/\sqrt{n}$, so $v_{e\|}/V_A \propto 1/\sqrt{n}$. Thus in our constant n model $v_{e\|}/V_A$ is not expected to vary significantly with latitude. An important property of our solution is the ability of $(v_{e\|}\nabla_\|)v_{e\|}$ to dominate $\omega v_{e\|}$ even when $v_{e\|}/V_A < 1$. This is a result of our nonuniform equilibrium model, a feature absent from many previous studies in which this behavior is not possible.

[38] The time dependence of the linear term ($\omega v_{e\|}$) will be oscillatory with the frequency of the Alfvén wave, and so the electric field at low latitudes (less than 8 R_E along the field line from the equator) will experience an $E_\|$ that switches sign. Sections of field line beyond this will be dominated by the $(v_{e\|}\nabla_\|)v_{e\|}$ term, and this will have a time dependence of, say, $\sin^2(\omega t)$ based upon the electron fluid description. This suggests that $E_\|$ does not switch sign in this region: It is always directed away from the Earth, although its magnitude will decrease to zero every half period of the Alfvén wave. In practice a consideration of the different electron populations may change this picture significantly, and in the following subsections we show how the introduction of an ionospheric electron population restricts the validity of the electron fluid model.

5.2. Effect of the Ionosphere

[39] Our analysis so far has used a fluid description for the electrons which yields an electron center-of-mass velocity $\mathbf{v}_e$. This can be a useful approximation when all the electrons are travelling with similar speeds or the population has a common drift velocity, but this is not always the case. For example, in the ionosphere (for the present purposes this may be taken to be the F region) observations show that the upward current (downgoing electrons) comprise an energetic (keV) beam of magnetospheric electrons passing through a background of essentially stationary ionospheric electrons. This situation is obviously not very well described by a single drifting electron population. In contrast, a downward ionospheric current (upgoing electrons) is carried by the abundant ionospheric electron population drifting in a highly collimated fashion along the magnetic field. Although observations show these electrons are not strictly mono-energetic [*Ergun et al.*, 1998], this electron motion may be described quite well by an electron fluid.

[40] The situation is reversed at higher altitudes beyond the accelerator region. Here the upward current (downgoing electrons) is carried by a drift of the magnetospheric electrons earthward, and should be described reasonably by our electron fluid model. However, a downward current in the outer magnetosphere is carried by an upgoing collimated beam of ionospheric electrons that can be observed to carry the current to the equatorial section. In this case the magnetospheric electrons play a minor role in carrying the current and are effectively stationary compared to the energetic beam of ionospheric electrons passing through them. This situation is similar to that encountered in the ionosphere during an upward current (downgoing electrons) and is not described well by an electron fluid.

[41] These remarks suggest that a simple two-fluid description is inadequate. *Rönnmark and Hamrin* [2000] have tried to address this issue by introducing one fluid for the magnetospheric electrons and another for the ionospheric ones (while retaining the usual ion fluid). The most satisfactory way to model currents in the F region is through using an electron distribution function, which is a formidable problem, and beyond the scope of the present article. However, it is possible to gain considerable insight into the behavior of upward and downward current carriers by thinking of magnetospheric and ionospheric electrons as separate species, and the observations above indicate how a distribution function solution can be expected to change the results of Figure 4, at least qualitatively.

[42] Why are field aligned currents sometimes carried by a population drifting as a whole, and at other times by an energetic beam passing through a background of almost stationary electrons? The answer has to do with the relative number densities of current carrying electrons (n_c) to equilibrium ions (n), and quasi-neutrality. (For the moment we assume that ions are sufficiently massive that they do not move appreciably during a wave cycle so the ions are fixed, and quasi-neutrality will then determine the total n_e at any point along the field line.)

5.2.1. Upward currents

[43] Consider the case of upward $j_\|$ (downgoing electrons) first. Initially the only $j_\|$ carriers in the magnetospheric section are magnetospheric electrons. These must drift earthward and may be accelerated by an $E_\|$ that acts equally on all electrons forming a downgoing electron beam. Thus, in the magnetosphere, $n_c \approx n$. The entire magnetospheric population drifts forming a beam and on approaching the Earth becomes more energetic since $n_c \approx n$ is constant (above the ionosphere), but $j_\|$ increases. This is just the situation we describe in our fluid formulation.

[44] The downgoing electrons can eventually emerge from the accelerator region and encounter the ionosphere, which we represent by a section of extent h where the equilibrium n at the base may be 10^{10} m^{-3} and falls off with a vertical scale height of 400 km. At an altitude of 0.5 R_E the ionospheric number density will have fallen to the magnetospheric value (10^6 m^{-3}), so $h \approx 0.5R_E$. Observations show that an upward current in the ionosphere continues to be carried by the downgoing magnetospheric electron beam which does not require further acceleration.

This can be understood by realising that in the ionosphere $n_c \ll n$, so quasi-neutrality does not impose a strong constraint on the density of the electron beam. Here quasi-neutrality will require very small adjustments to the abundant equilibrium ionospheric electron distribution to compensate for the introduction of the magnetospheric electron beam. This can be achieved with a very small $E_\parallel$ (much less than that in the accelerator region) which will act on ionospheric and magnetospheric electrons alike, but is not large enough to change the beam's energy significantly.

[45] The increase of $j_\parallel$ across the F region by a factor of 2 or 3 can be met without any further energization of the magnetospheric beam: since quasi neutrality does not determine its density here, the natural focussing effect of the converging field lines alone will increase the beam's n_c and $j_\parallel$ by exactly the right amount. Figure 5a summarises the situation for the downgoing magnetospheric electrons: They are accelerated in the magnetospheric section, as described earlier, to form a high energy beam. The $E_\parallel$ over the ionospheric section is so small that, from an observational point of view, $E_\parallel$ would appear to fall to zero in the F region, while an energetic beam of magnetospheric electrons passes through an essentially stationary ionospheric plasma distribution. The electric field in Figure 5a is in accord with *Rönnmark*'s [1999] comment that there is a negligible potential drop ($\int E_\parallel d\ell$) over the height of the ionosphere for an upward current. Figure 5a explicitly depicts the two types of electrons that exist during the upward current phase, and reinforces our earlier claim that a single electron fluid is inadequate here.

5.2.2. Downward currents

[46] As the Alfvén wave cycle proceeds, the current density falls to zero before switching to a downward current. Figure 5b shows the variation of $E_\parallel$ and $v_{e\parallel}$ over the last few R_E of the field line at the moment of maximum downward current (upgoing electrons). During the downward current phase magnetospheric electrons are not an important current carrier in the F region. The current is carried over the lower F region by a slow upward drift of plentiful ionospheric electrons, which are accelerated by a small downward $E_\parallel$. In this situation $n_c \approx n$, so the upward motion of the ionospheric electrons should be described reasonably by the fluid approximation given earlier. The ion density falls off with height, and quasi-neutrality will require the electron density to decrease similarly. Consequently the slow upward drift of electrons must increase in speed as they move to the upper (less dense) part of the F region. The downward $E_\parallel$ will thus increase with altitude through the F region. At the top of the F region (which we take to be the point where the ionospheric and magnetospheric electron number densities are equal) the ionospheric electrons must be accelerated to similar energies as the downgoing magnetospheric electron beam that carried the current at this point half a cycle earlier [e.g., *Rönnmark*, 1999], and will require a sharp spike of downward $E_\parallel$ which, in our model, occurs in the upper layer of the ionosphere. This feature is also consistent with the strong gradient in potential at the magnetosphere/ionosphere boundary found by *Temerin and Carlson* [1998] (see their Figure 1). Observations of upgoing electrons by *Ergun et al.* [1998] show their energy agrees remarkably well with the inferred parallel potential ($\int E_\parallel d\ell$) and confirms the importance of the downward $E_\parallel$ spike in Figure 5b. They also show that although the electrons are highly collimated, they can have a rather broad energy spectrum and are not monoenergetic.

[47] Once the upgoing electrons leave the top of the ionosphere as a beam n_c will decrease in proportion to B because of the diverging field lines, and soon $n_c \ll n$. Using the same ideas as before we conclude that a very small $E_\parallel$ will exist beyond altitudes of the order of an R_E whose main role is to shift the more plentiful magnetospheric electrons slightly so that quasi-neutrality is satisfied as the relatively diffuse beam of ionospheric electrons arrives. The $E_\parallel$ over the magnetospheric section will be so small compared to that at the top of the ionosphere (see Figure 5b) that the energy of the beam of ionospheric electrons is not changed significantly, and the fall off of $j_\parallel$ with altitude will arise naturally from the diverging electron trajectories.

[48] Although we apply similar ideas to the up and downgoing electron beams characterised by the value of n_c/n, it should be noted that there may be considerable asymmetry in the two beams as a result of the different background electron temperatures and n/B scale heights above and below the acceleration region.

[49] It is interesting to compare the modified $E_\parallel$ we propose in Figures 5a and 5b with that found by *Rönnmark and Hamrin* [2000]. Their calculation was for a steady current system which contained an upward current on one set of field lines and a downward current on an adjacent set. Their Figure 4b is a surface plot of the variation of $E_\parallel$ in a meridian plane. If we take two slices through this surface along the field lines carrying the maximum upward and downward currents we find the variation of $E_\parallel$ is qualitatively the same as that shown in our Figures 5a and 5b, and gives credence to the modifications we have introduced to the single electron fluid model.

5.3. Parallel Ion Motion

[50] Although we have considered ions to have negligible field-aligned motion on the electron and Alfvén timescales, it is possible that over several cycles, or in the case of a steady current ($\omega \to 0$), that there could be a significant change in the ion distribution. For example, *Temerin and Carlson* [1998] note that although the downward $E_\parallel$ spike (Figure 5b) is required to accelerate a beam of ionospheric electrons out into the magnetosphere, it will also have the effect of causing the ions there to drift earthward. *Ergun et al.*'s [1998] observations show that during the upward current phase (Figure 5a) the energy of the upward ion beam is in excellent agreement with the parallel potential (inferred from $\mathbf{E}_\perp$ measurements), and supports the existence of the upward $E_\parallel$ we describe.

[51] Curiously, upgoing ions are also observed in regions of downward current. We might anticipate that the downward $E_\parallel$ spike in Figure 5b would move ionospheric ions downward. However, *Temerin and Carlson* [1998] note that the intense waves that are generally observed in regions of strong current will heat the ion's perpendicular to **B**, and the resulting mirror force will act to balance the downward $E_\parallel$ force allowing the possibility of maintaining a significant ion density here. *Lund et al.* [1999] also advocate the role of the downward $E_\parallel$ spike in downward currents by claiming that it is required to explain their FAST observations of ion

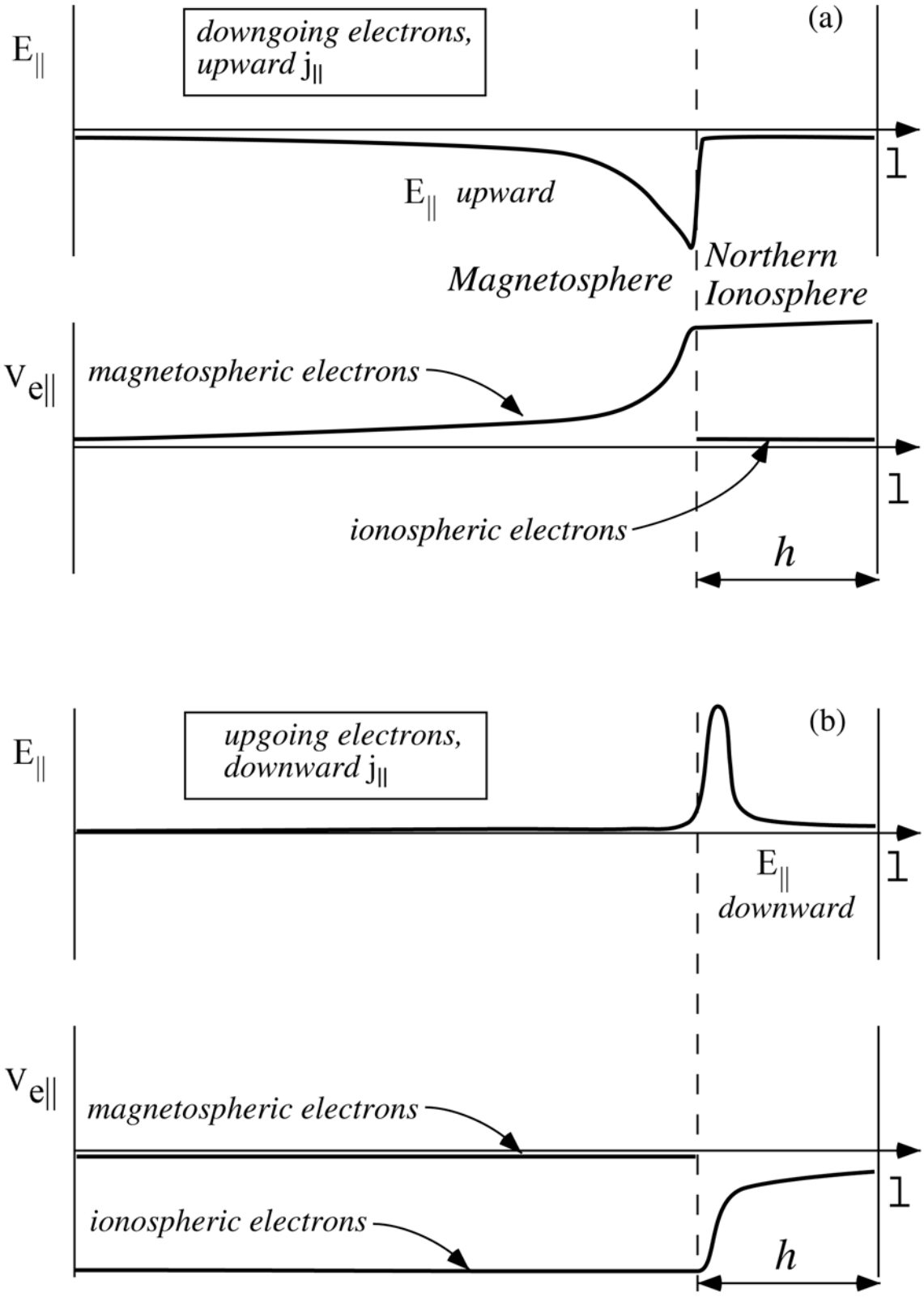

Figure 5. The variation of $E_{\|}$ (upper panel) and $v_{e\|}$ (lower panel) over the last few R_E of the field line at the northern ionosphere at times of (a) maximum upward current and (b) maximum downward current.

conics: They reported H^+, He^+ and O^+ ions at 3000 km altitude for which ion energies were mass independent. Wave-ion heating mechanisms alone will not give this result. However, their calculations suggest that the downward $E_{\|}$ acts to trap the ions in the heating region from which they can eventually emerge with similar energies.

[52] The mechanisms described above may contribute to the formation of ionospheric density cavities which are

common on auroral current field lines, and can have densities similar to those in the magnetosphere (10^6 m^{-3}) and sometimes less [*Strangeway et al.*, 1998]. During the formation of such cavities, we could represent the situation by reducing n and h (in Figure 5). The limit of complete evacuation of ionospheric material would be represented by $h \rightarrow 0$, and this is the situation described in Figure 4. Thus the upward current $E_\parallel$ based on Figure 4 of 1 mVm^{-1} is open to revision, as it is determined by $v_{e\parallel}$ which is dependent upon $j_\parallel$ and n. Using equation (22) we rewrite equation (30) to leading order in m_e/m_i over the magnetospheric section as

$$E_\parallel \approx -\frac{m_e}{ne^3}(j_\parallel \nabla_\parallel)\left(\frac{j_\parallel}{n}\right) \tag{35}$$

During upward currents the point on the magnetospheric side of the magnetosphere-ionosphere boundary (the dashed line in Figure 5a) will have the greatest upward $E_\parallel$, and is almost coincident with the peak of B/n. Thus a nonzero h will mean the upward $E_\parallel$ magnitude estimated from Figure 4 needs to be decreased. For example, taking the maximum value of h to be 0.5 R_E will reduce the upward $E_\parallel$ to 0.1 mVm^{-1}. (This can be regarded as a lower limit.) On the other hand, since $E_\parallel \propto 1/n^2$, an efficient evacuation of the ionosphere to $n = 0.3 \times 10^6$ m^{-3} could produce $E_\parallel = 10$ mVm^{-1}. The two effects may compensate for one another, and it is expected that a partially evacuated ionosphere should be able to support an $E_\parallel$ of the order of 1 mVm^{-1}. This seems an inescapable conclusion if electrons with an energy of $\sim$1 keV, as are commonly observed, are accelerated over distances of the order of an Earth radius.

5.4. Observations

[53] It would be interesting to look directly for the upward directed electric field we expect to exist above the ionosphere during the upward current phase (Figure 5a), although it is not normally possible to resolve $E_\parallel$ in spacecraft data. *Mozer and Kletzing* [1998] report 4 large amplitude events where a direct measurement of $E_\parallel$ was possible. They conform to our expectations, and are all for downgoing electrons (upward current). This may well be no coincidence since our model suggests that there will not be a significant $E_\parallel$ at high altitudes for upgoing electrons (downward currents) - see Figure 5b. It may be that the effects of $E_\parallel$ will often be easier to observe than the field itself. It would cause a secular drift of ions from high latitudes away from earth, and may contribute to the distribution of oxygen ions throughout the magnetosphere, or play a role in producing the density cavities observed at high latitudes. Indeed the process could be unstable: A small upward $E_\parallel$ would cause the drift of ions to higher altitudes. This would lower n locally, requiring the remaining charge carriers to move faster to carry the current. If the electrons are to move faster they must experience a larger $E_\parallel$ (equation (35)), and this will cause a larger drift of ions to high altitudes which will reduce n further, and so on. Of course, the ponderomotive force of ULF waves can also cause the removal of material from high latitudes [*Allan* 1993a, 1993b], although the material at the end of the field line requires a push to get started [*Allan*, 1993b], and this could be provided by the $E_\parallel$ our calculation predicts.

[54] We also noted in the previous subsection that ion heating (while trapped by the downward $E_\parallel$ spike of Figure 5b) can also lead to ion outflows. Thus it seems possible that both upward and downward $E_\parallel$ regions will lead to an erosion of the top of the ionosphere.

5.5. Future Studies

[55] Our model contains many simplifications that should be addressed in future calculations. For example, the E region has been taken as perfectly conducting, so there is no dissipation in our model. This is probably not too serious as *Rönnmark* [1999] shows that $E_\parallel$ is fairly insensitive to the height-integrated Pedersen conductivity. Our equilibrium model assumed a constant n along the field line in accord with observations. Future work will see how efficiently the processes described above can evacuate the high latitude section of the field line. Our analytical model focuses on the current carrying properties of the magnetospheric section of the circuit. An important advance will be to include the interaction of the down-going electron beams with the ionosphere, of which we have attempted to describe the principal features qualitatively in Figure 5a. For example, *Rönnmark* [1999] suggests that the downgoing electron beam leaving the accelerator region will remain at high energy and carry the current to the E region. The F region electron population, whose number density greatly exceeds that of the accelerated magnetospheric electron beam, could play a minor role in carrying the current. This is not thought to be true of a downward F region current where the only available charge carriers are upward moving ionospheric electrons, which will need to be accelerated. This suggests there could be an asymmetry in the upward and downward current regions. This asymmetry may be why *Mozer and Kletzing* [1998] could only measure $E_\parallel$ in down-going electron events. Perhaps the magnetospheric $E_\parallel$ of up-going electrons is somewhat reduced. However, such effects are not represented by the two-fluid equations, and will require a kinetic treatment or consideration of test particle dynamics to clarify these issues which we have only addressed qualitatively in this section.

[56] The other notable simplification in our model is the neglect of plasma pressure. When this is included the particles will experience a mirror force causing a reduction in the number of charge carriers at high latitude for downgoing electrons [*Rankin et al.*, 1999]. Consequently, the reduced number of electrons that can access high latitudes will have to travel faster to carry the current there, and require an enhanced $E_\parallel$. Again, this may be related to *Mozer and Kletzing*'s [1998] bias for observing $E_\parallel$ associated with down-going rather than up-going electron beams.

6. Summary

[57] We have presented a model for ULF FLRs in a dipole magnetosphere. In such a geometry the current density increases significantly at high latitudes and electrons need to have energies of keV to carry observed current densities. Retaining electron inertia, we find that parallel electric fields of mVm^{-1} are required, and that most of the acceleration occurs 1 or 2 R_E above the ionosphere.

[58] Our calculation began with a leading order solution corresponding to a single fluid Alfvén wave in which m_e/m_i

and ω/ω_{ci} were neglected. This is the same approximation that has proved to be so successful over the last 5 decades when explaining the properties of ULF waves. We have refined this description by calculating the correction to the solution when the neglected terms are retained, and most of our effort has been focused on the electrons. The dynamics of keV electrons is nonlinear and the inappropriate neglect of nonlinear terms from the electron momentum equation leads to a serious underestimate of the associated parallel electric field by several orders of magnitude.

[59] The physical processes described in this paper can provide an explanation for the electron acceleration in FLRs to keV energies over a 1 R_E scale above the ionosphere. Similar energization is often discussed in terms of an ''accelerator region'' in other contexts and it is likely that the processes we describe here will operate in many other auroral current circuits or where optical auroral emissions are produced. For example, *Allan and Wright* [2000] showed that Alfvén waves propagating Earthward in the plasma sheet boundary layer had the spatial structure required to explain observed equatorward-propagating auroral forms described by *Liu et al.* [1995] and *Wright et al.* [1999]. However, their single-fluid MHD model could not explain the electron acceleration necessary to produce visible aurorae. It seems likely that the electron acceleration mechanism described here will provide the energies required in the *Allan and Wright* [2000] propagating wave model just as it does in the standing wave model adopted in this paper.

Appendix

[60] In this section we summarise the analytic solution for linear axisymmetric toroidal Alfvén waves in a dipole equilibrium field geometry given by *Taylor and Walker* [1984]. They derived a family of solutions for a density variation proportional to r^{-p}. For our uniform density model we set $p = 0$. In terms of the latitude (θ) and geocentric radial distance (r) the dipolar coordinates (ν, ϕ, μ) are $\nu = -\cos^2\theta/r$, $\mu = \sin\theta/r^2$, and ϕ is the usual azimuthal coordinate. The scale factors of the dipole coordinates are $h_\nu = r^2/(\cos\theta\sqrt{1+3\sin^2\theta})$, $h_\phi = r\cos\theta$, and $h_\mu = r^3/\sqrt{1+3\sin^2\theta}$. Along a field line $r = LR_E\cos^2\theta$. The wave equation may be written

$$\frac{d^2\varepsilon_\nu}{dz^2} + k^2(1-z^2)^{6-p}\varepsilon_\nu = 0 \tag{36}$$

where field aligned derivatives are expressed in terms of $z = \sin\theta$, $\varepsilon_\nu = h_\nu E_\nu$, $k = \omega LR_E/V_{A0}$, L is the L value of the field line, and V_{A0} is the equatorial Alfvén speed on the field line. We shall only consider the fundamental solution, and this will be symmetric about the equator, while perfectly reflecting ionospheres give nodes ($\varepsilon_\nu = 0$) at $\theta = \pm\Lambda$, where Λ is the invariant latitude.

[61] Parameterising in terms of the coordinate $s = z + z_0$, where $z_0 = \sin\Lambda$, equation (36) may be cast in the standard form

$$\frac{d^2\varepsilon_\nu}{ds^2} + k^2(1-\eta(s))\varepsilon_\nu = 0 \tag{37}$$

where $\eta(s) = 1 - (1 - (s - s_0/2)^2)^{6-p}$, and $s_0 = 2z_0$. *Taylor and Walker*'s [1984] solution is expressed as a perturbation series expansion in terms of the eigenfunctions (Φ_n) and eigenfrequencies (k_n) of the $\eta = 0$ equation,

$$\frac{d^2\Phi_n}{ds^2} + k_n^2\Phi_n = 0 \tag{38}$$

The normalized eigenfunctions and eigenvalues are

$$\Phi_n = \sqrt{\frac{2}{s_0}}\sin\left(\frac{n\pi s}{s_0}\right), \quad n = 1, 2, 3\ldots \tag{39}$$

$$k_n^2 = \left(\frac{n\pi}{s_0}\right)^2, \quad n = 1, 2, 3\ldots \tag{40}$$

The first-order expressions for the fundamental eigenfunctions and eigenvalues of our problem equation (37) are

$$\varepsilon_1 = \Phi_1 + \frac{\eta_{13}}{9\eta_{11} - 8}\Phi_3 \tag{41}$$

$$k^2 = \frac{k_1^2}{1 - \eta_{11}} \tag{42}$$

(Note that we have truncated the series in equation (41) at the third Fourier coefficient.) The parameters η_{nm} are defined as

$$\eta_{nm} = \int_0^{s_0} \Phi_m(s)\eta(s)\Phi_n(s)ds \tag{43}$$

The evaluation of η_{nm} is straightforward, but very lengthy: $\eta(s)$ is given in terms of a sum of integrals of powers of s and sine functions which are of standard form. However, we would not recommend that their evaluation be attempted by hand, and advise the task be performed by a symbolic computation package. The algebra runs to many sheets of calculation, and it is almost inevitable that even the most diligent worker is likely to make a slip in addition to taking inordinately longer than a computer.

[62] After integration we obtained η_{11} and η_{13} as polynomials in s_0 of the form $a_2 s_0^2 + a_4 s_0^4 + a_6 s_0^6 + \ldots + a_{12} s_0^{12}$. (The exact number of terms depends upon the index p, but it is of this form for $p = 0$.) The coefficients a_n are conveniently given as numbers for a particular p, as are η_{nm} for a given Λ and p. Again, we recommend that they be evaluated using Maple or Mathematica, since it is difficult to work to a consistent accuracy throughout the manipulations if done by hand. For the $p = 0$ model relevant to the main text in our paper we find for η_{11}, $a_2 = 0.196036449$, $a_4 = -0.038530162$, $a_6 = 0.005603641$, $a_8 = -5.48857 \times 10^{-4}$, $a_{10} = 3.2172 \times 10^{-5}$, $a_{12} = -8.51 \times 10^{-7}$; and for η_{13}, $a_2 = 0.227972663$, $a_4 = -0.068417765$, $a_6 = 0.011948990$, $a_8 = -1.293119 \times 10^{-3}$, $a_{10} = 8.0578 \times 10^{-5}$, $a_{12} = -2.221 \times 10^{-6}$. The neglect of the 5th harmonic term in (41) is a good approximation for our model since its amplitude is significantly less than the third harmonic ($\eta_{15}/\eta_{13} \sim 0.1$). For the $L = 10$ field line used in the main text $\Lambda = 71.54°$, $\eta_{11} = 0.3932$, and $\eta_{13} = 0.3182$.

[63] *Taylor and Walker* [1984] comment that their approximation is significantly better than the WKB approximation, and they are right. For example, their Figure 1 shows the error in the eigenvalue is always less than 2% compared to almost

10% for the WKB method. Their Figure 4 compares the exact (numerical) eigenfunction with that predicted by their series expansion and the WKB method for $p = 2$ and $\Lambda = 64°$. (For this equilibrium and field line we calculate $\eta_{11} = 0.2952$ and $\eta_{13} = 0.2766$.) Comparing the functions (normalised to unity at $\theta = 0$) at $\sin\theta = 0.5$ with the exact answer (0.5737), the WKB method (0.413) has an error of almost 30%, whereas the Taylor and Walker approximation (0.628) has an error of only 10%. Interestingly, our formula equation (41) is slightly different to Taylor and Walker's expression since we estimated the coefficient of the third harmonic to slightly greater accuracy. (See the original treatment of *Morse and Feschbach* [1953, equation (9.1.10)].) Our expression gives 0.5676, which has an error of only 1%. In hindsight, we can see that evaluating the a_j coefficients to the seventh decimal place will guarantee that rounding errors are not significant. (Note that the maximum possible value of s_0^{12} is approximately 4000.)

[64] Returning to the $L = 10$ field line with $p = 0$ as used in the main part of the paper, we can estimate the equatorial Alfvén speed in terms of the definition of k following equation (36) and our estimate for it using equations (40) and (42). If the fundamental mode has a frequency of 2 mHz, the equatorial Alfvén speed will be 400 km s^{-1}.

[65] When considering an FLR or Alfvén wave extending across a range of L shells it is important to realise that the eigenfunctions will vary slightly with L shell. However, for a narrow resonance whose width in L is less than that on which the eigenfunctions vary, we can say the eigenfunctions are approximately independent of L in our region of interest. Thus

$$E_\nu(\nu,\mu) \approx f(\nu)\varepsilon_1(\nu_0,\mu)/h_\nu \tag{44}$$

and the spatial variation in ν is described by the envelope $f(\nu)$. (The position ν_0 labels the field line on which our interest is focussed.) This is just the form found in studies that have derived Frobenius series solutions about a resonant dipole field line for steadily driven FLRs [e.g., *Wright and Thompson*, 1994]. The same approximation has also been used by *Walker* [1980]. The amplitude of the envelope function $f(\nu)$ is such that it gives the FLR amplitude and cross L-shell scale discussed at the end of section 1. (The exact details of f are not important for the present calculation, but $|f| \approx 4 \times 10^{12}$ Vm, and $\Delta\nu \approx 4 \times 10^{-10}$ m^{-1}). The leading order v_ϕ is found easily from the ν component of equation (15), $v_\phi = -E_\nu/B$, and the field aligned variation is given explicitly in equation (32). The Alfvén wave magnetic field is given by the ϕ component of equation (13), which may be written

$$i\omega b_\phi = \frac{1}{h_\nu}\frac{d(h_\nu E_\nu)}{d\ell} \tag{45}$$

Here, $d/d\ell$ refers to the field aligned derivative ($\nabla_\parallel$) which is given by $(1/h_\mu)\partial/\partial\mu$ in the dipole coordinates. It is often convenient to parameterise this derivative in terms of θ,

$$\frac{d}{d\ell} = \frac{1}{LR_E\cos\theta\sqrt{1+3\sin^2\theta}}\frac{d}{d\theta} \tag{46}$$

When it is necessary to take the field aligned derivative of $\varepsilon_1(s)$ the chain rule should be used

$$\frac{d}{d\ell} = \frac{d\theta}{d\ell}\frac{ds}{d\theta}\frac{d}{ds} \tag{47}$$

noting that $ds/d\theta = \cos\theta$.

[66] Equation (46) may be integrated to give the distance along the field line (from the equatorial plane) in terms of θ

$$\ell = LR_E\left(\frac{1}{2}\sin\theta\sqrt{1+3\sin^2\theta} + \frac{\sqrt{3}}{6}\sinh^{-1}\left(\sqrt{3}\sin\theta\right)\right) \tag{48}$$

This expression, in conjunction with the identity $\sinh^{-1}z = \ln(z+\sqrt{z^2+1})$, was used in Figure 4. The parallel current follows directly from b_ϕ using equations (14), (41), (44) and (45). After some algebra we find

$$j_\parallel \approx \frac{\pi}{i\omega L^5 R_E^2 s_0 \mu_o}\frac{df(\nu)}{d\nu}\frac{\sqrt{1+3\sin^2\theta}}{\cos^6\theta}\sqrt{\frac{2}{s_0}}\left(\cos\left(\frac{\pi s}{s_0}\right) + \frac{3\eta_{13}}{9\eta_{11}-8}\cos\left(\frac{3\pi s}{s_0}\right)\right) \tag{49}$$

and using equation (22) the field aligned variation of $v_{e\parallel}$ may be shown to obey equation (31). The calculation of the three acceleration terms in equation (29) is now straightforward using the results of this appendix.

[67] **Acknowledgments.** A. N. W. is supported through a U.K. PPARC Advanced Fellowship. M. S. Ruderman was supported by a U.K. PPARC Research Grant at the University of St. Andrews during the course of this work. A. N. W. is grateful to NIWA for their hospitality during the visit over which most of this work was done, and is grateful to J. McFadden, F. Mozer, T. Neukirch, K. Rönnmark, K. Shiokawa, and R. Strangeway for helpful discussions. R. Strangeway also developed the code used to analyse the FAST magnetometer data.

[68] Michel Blanc thanks the referee for his assistance in evaluating this paper.

References

Alfvén, H., On the theory of magnetic storms and aurorae, *Tellus*, *10*, 104, 1958.

Allan, W., The ponderomotive force of standing Alfvén waves in a dipolar magnetosphere, *J. Geophys. Res.*, *98*, 1409, 1993a.

Allan, W., Plasma energization by the ponderomotive force of magnetospheric standing Alfvén waves, *J. Geophys. Res.*, *98*, 11,383, 1993b.

Allan, W., and A. N. Wright, Magnetotail waveguide: Fast and Alfvén waves in the plasma sheet boundary layer and lobe, *J. Geophys. Res.*, *105*, 317, 2000.

Bryant, D. A., Electron acceleration in the aurora, *Contemp. Phys.*, *35*, 165, 1994.

Bryant, D. A., A. C. Cook, Z.-S. Wang, U. de Angelis, and C. H. Perry, Turbulent acceleration of auroral electrons, *J. Geophys. Res.*, *96*, 13,829, 1991.

Bryant, D. A., R. Bingham, and U. de Angelis, Double layers are not particle accelerators, *Phys. Rev. Lett.*, *68*, 37, 1992.

Dungey, J. W., *Cosmic Electrodynamics*, p. 36, Cambridge Univ. Press, New York, 1958.

Ergun, R. E., et al., FAST satellite observations of electric field structures in the auroral zone, *Geophys. Res. Lett.*, *25*, 2025, 1998.

Goertz, C. K., and R. W. Boswell, Magnetosphere-ionosphere coupling, *J. Geophys. Res.*, *84*, 7239, 1979.

Hasegawa, A., Particle acceleration by MHD surface waves and formation of the aurora, *J. Geophys. Res.*, *81*, 5083, 1976.

Knight, S., Parallel electric fields, *Planet. Space Sci.*, *21*, 741, 1973.

Liu, W. W., B.-L. Xu, J. C. Samson, and G. Rostoker, Theory and observations of auroral substorms: A magnetohydrodynamic approach, *J. Geophys. Res.*, *100*, 79, 1995.

Lund, E. J., et al., Mass-dependent effects in ion conic production: The role of parallel electric fields, *Geophys. Res. Lett.*, *26*, 3593, 1999.

Lysak, R. L., and M. K. Hudson, Coherent anomalous resistivity in the region of electrostatic shocks, *Geophys. Res. Lett.*, *6*, 661, 1979.

Mann, I. R., A. N. Wright, and P. S. Cally, Coupling of magnetospheric cavity modes to field line resonances: A study of resonance widths, *J. Geophys. Res.*, *100*, 19,441, 1995.

Morse, P. M., and H. Feshbach, *Methods of Theoretical Physics*, McGraw-Hill, New York, 1953.

Mozer, F. S., and C. A. Kletzing, Direct observation of large, quasi-static, parallel electric fields in the auroral acceleration region, *Geophys. Res. Lett.*, *25*, 1629, 1998.

Mozer, F. S., C. W. Carlson, M. K. Hudson, R. B. Torbert, B. Parady, J. Yatteau, and M. C. Kelley, Observations of paired electrostatic shocks in the polar magnetosphere, *Phys. Rev. Lett.*, *38*, 292, 1977.

Nakamura, T. K., Parallel electric field of a mirror kinetic Alfvén wave, *J. Geophys. Res.*, *105*, 10,729, 2000.

Rankin, R., J. C. Samson, and V. T. Tikhonchuk, Electric fields in dispersive shear Alfvén waves in the dipolar magnetosphere, *Geophys. Res. Lett.*, *26*, 3601, 1999.

Rönnmark, K., Electron acceleration in the auroral current circuit, *Geophys. Res. Lett.*, *26*, 983, 1999.

Rönnmark, K., and M. Hamrin, Auroral electron acceleration by Alfvén waves and electrostatic fields, *J. Geophys. Res.*, *105*, 25,333, 2000.

Samson, J. C., T. J. Hughes, F. Creutzberg, D. D. Wallis, R. A. Greenwald, and J. M. Ruohoniemi, Observations of a detached, discrete arc in association with field line resonances, *J. Geophys. Res.*, *96*, 15,683, 1991.

Samson, J. C., D. D. Wallis, T. J. Hughes, F. Creutzberg, J. M. Ruohoniemi, and R. A. Greenwald, Substorm intensifications and field line resonances in the nightside magnetosphere, *J. Geophys. Res.*, *97*, 8495, 1992.

Samson, J. C., L. L. Cogger, and Q. Pao, Observations of field line resonances, auroral arcs and auroral vortex structures, *J. Geophys. Res.*, *101*, 17,373, 1996.

Strangeway, R. J., et al., FAST observations of VLF waves in the auroral zone: Evidence of very low plasma densities, *Geophys. Res. Lett.*, *25*, 2065, 1998.

Streltsov, A., and W. Lotko, The fine structure of dispersive, nonradiative field line resonance layers, *J. Geophys. Res.*, *101*, 5343, 1996.

Streltsov, A., and W. Lotko, Dispersive, nonradiative field line resonances in a dipolar magnetic field geometry, *J. Geophys. Res.*, *102*, 27,121, 1997.

Streltsov, A., W. Lotko, J. R. Johnson, and C. Z. Cheng, Small-scale, dispersive field line resonances in the hot magnetospheric plasma, *J. Geophys. Res.*, *103*, 26,559, 1998.

Swift, D. W., On the formation of auroral arcs and acceleration of auroral electrons, *J. Geophys. Res.*, *80*, 2096, 1975.

Swift, D. W., Mechanisms for the discrete aurora - A review, *Space Sci. Rev.*, *22*, 35, 1978.

Taylor, J. P. H., and A. D. M. Walker, Accurate approximate formulae for toroidal standing hydromagnetic oscillations in a dipolar geomagnetic field, *Planet. Space Sci.*, *32*, 1119, 1984.

Temerin, M., and C. W. Carlson, Current-voltage relationship in the downward auroral current region, *Geophys. Res. Lett.*, *25*, 2365, 1998.

Walker, A. D. M., Modelling of Pc5 pulsation structure in the magnetosphere, *Planet. Space Sci.*, *28*, 213, 1980.

Wei, C. Q., J. C. Samson, R. Rankin, and P. Frycz, Electron inertial effects on geomagnetic field line resonances, *J. Geophys. Res.*, *99*, 11,265, 1994.

Wright, A. N., MHD theory of magnetic pulsations, in *Physical Signatures of Magnetospheric Boundary Layer Processes*, edited by J. A. Holtet and A. Egeland, p. 329, Kluwer Acad., Norwell, Mass., 1994a.

Wright, A. N., Dispersion and wave coupling in inhomogeneous MHD waveguides, *J. Geophys. Res.*, *99*, 159, 1994b.

Wright, A. N., and W. Allan, Are two-fluid effects relevant to ULF pulsations?, *J. Geophys. Res.*, *101*, 24,991, 1996.

Wright, A. N., and M. J. Thompson, Analytical treatment of Alfvén resonances and singularities in nonuniform magnetoplasmas, *Phys. Plasmas*, *1*, 691, 1994.

Wright, A. N., W. Allan, R. D. Elphinstone, and L. L. Cogger, Phasemixing and phase motion on tail-like and dipole-like magnetic field lines, *J. Geophys. Res.*, *104*, 10,159, 1999.

Xu, B.-L., J. C. Samson, W. W. Liu, F. Creutzberg, and T. J. Hughes, Observations of optical aurora modulated by resonant Alfvén waves, *J. Geophys. Res.*, *98*, 11,531, 1993.

W. Allan, National Institute of Water and Atmospheric Research, P. O. Box 14-901, Kilbirnie, Wellington, New Zealand. (w.allan@niwa.cri.nz)

R. C. Elphic, Space and Atmospheric Sciences Group, MS D466, Los Alamos National Laboratory, Los Alamos, NM 87545, USA. (relphic@lanl.gov)

M. S. Ruderman, Department of Applied Mathematics, University of Sheffield, Hicks Building, Western Bank, Sheffield, S3 7RH, England, UK. (M.S.Ruderman@sheffield.ac.uk)

A. N. Wright, Mathematical Institute, University of St. Andrews, St. Andrews, Fife KY16 9SS, Scotland, UK. (andy@mcs.st-and.ac.uk)